Universidad de Cantabria

Facultad de Ciencias

ON LIGHT SCATTERING BY NANOPARTICLES WITH CONVENTIONAL AND NON-CONVENTIONAL OPTICAL PROPERTIES

PH.D. THESIS

Braulio García-Cámara

Santander, July 2010

4

Directionality of the Scattered Light by an Isolated Particle

"No hay que olvidar que cuando se descubrió el radio, nadie sabía que resultaría útil en los hospitales. El trabajo era ciencia pura. Y esto es una prueba de que el trabajo científico no debe considerarse desde el punto de vista de la utilidad directa de la misma"
—Marie Curie, 1867-1934, física polaca

4.1. Introduction

New applications in nanophotonics could be given interesting functionalities if one could control the way these structures distribute the scattered light in space. Several years ago, M. Kerker, D. Wang and C. Giles showed that for dipole-like particles with certain values of their optical properties, the scattering can be suppressed in certain directions and enhanced in others. Kerker's study was presented for ideal point particles with dimensions negligible compared to the incident wavelength. In this chapter, we present a formal study of the conditions for ϵ and μ as proposed by the former authors as well as a generalization to finite-size particles. Finally a generalization to other scattering directions will also be presented.

4.2. Kerker's Theory

In the early eighties, M. Kerker and co-authors [69] presented an interesting study about the scattering properties of particles with magnetic permeability ($\mu \neq 1$). More specifically, the authors considered a spherical particle much smaller than the incident wavelength, illuminated by a plane wave and without any restriction for the values of its optical constants (ϵ and μ). Some unusual electromagnetic scattering effects were described in this work such as the zero-backward and the zero-forward scattering. When they presented this study, just as when V. Veselago presented his results about the double-negative (DNG) materials [138], the idea of a magnetic permeability different from 1 in the visible range was hypothetical and the described effects were thought to be impossible to be observed. However, nowadays, the engineered metamaterials have revitalized these studies [148].

In this section we will briefly review the theoretical aspects described by M. Kerker et al [69].

4.2.1. Zero-Backward Scattering

When we considered a homogeneous and isotropic sphere of radius R and refractive index m embedded in a homogeneous and isotropic medium illuminated by a polarized plane wave of wavelength λ, the scattered intensity components can be written as [14]

$$I_{TE} = \frac{\lambda^2}{4\pi r^2} |S_1|^2 \sin^2 \phi \qquad I_{TM} = \frac{\lambda^2}{4\pi r^2} |S_2|^2 \cos^2 \phi \tag{4.1}$$

where r is the distance from the particle to the observer, ϕ is the angle between the incident electric field vector and the scattering plane, I_{TE} and I_{TM} are the two polarized components of the scattered intensity, with the electric field parallel and perpendicular to the scattering plane, respectively and S_1 and S_2 are the scattered field amplitudes that are described using Mie theory in (2.46) and (2.47) respectively.

When substituting the expressions of S_1 and S_2 [14] in equation (4.1), the scattered intensity components are given by

$$I_{TE} = \frac{\lambda^2}{4\pi r^2} \left| \sum_n \frac{2n+1}{n(n+1)} (a_n \pi_n + b_n \tau_n) \right|^2 \sin^2 \phi \qquad (4.2)$$

$$I_{TM} = \frac{\lambda^2}{4\pi r^2} \left| \sum_n \frac{2n+1}{n(n+1)} (a_n \tau_n + b_n \pi_n) \right|^2 \cos^2 \phi \qquad (4.3)$$

where the angular dependence in the scattering plane is represented by the functions π_n and τ_n defined in equation (2.48). If the considered particle can be conceived as a dipole-like particle, fulfilling the two conditions exposed in chapter 2, the previous expressions can be reduced to

$$I_{TE} = \frac{\lambda^2}{4\pi r^2} x^6 \left| \left(\frac{\epsilon - 1}{\epsilon + 2} \right) + \left(\frac{\mu - 1}{\mu + 2} \right) \cos(\theta) \right|^2 \sin^2 \phi \qquad (4.4)$$

$$I_{TM} = \frac{\lambda^2}{4\pi r^2} x^6 \left| \left(\frac{\epsilon - 1}{\epsilon + 2} \right) \cos(\theta) + \left(\frac{\mu - 1}{\mu + 2} \right) \right|^2 \cos^2 \phi \qquad (4.5)$$

For the backward direction ($\theta = 180°$) the previous expressions adopt the following forms

$$I_{TE}(180°) = \frac{\lambda^2}{4\pi r^2} x^6 \left| \left(\frac{\epsilon - 1}{\epsilon + 2} \right) - \left(\frac{\mu - 1}{\mu + 2} \right) \right|^2 \sin^2 \phi \qquad (4.6)$$

$$I_{TM}(180°) = \frac{\lambda^2}{4\pi r^2} x^6 \left| - \left(\frac{\epsilon - 1}{\epsilon + 2} \right) + \left(\frac{\mu - 1}{\mu + 2} \right) \right|^2 \cos^2 \phi \qquad (4.7)$$

From these expressions, it is easy to show that when $\epsilon = \mu$, the two terms between bars are equal but with different signs and hence, the scattered intensity in the backward direction is zero for both incident polarizations. As an example, in figure 4.1 the angular distribution of the scattered intensity is shown for a dipole-like particle with optical properties, $\epsilon = \mu = 3$. Only a TM polarization is considered because, as it will be explained, the scattered intensity is equal for both polarization under Kerker's condition.
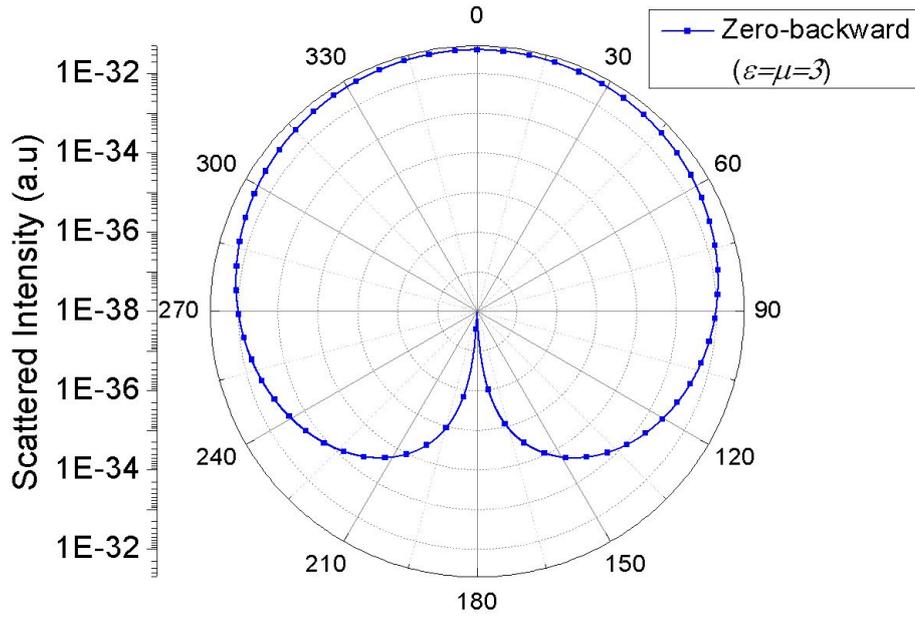
Figure 4.1: Scattering diagram for a dipole-like particle ($R = 10^{-6}\lambda$) with optical properties fulfilling the zero-backward condition and for a TM incident polarization

4.2.2. Zero-Forward Scattering

Now, we consider the forward direction ($\theta = 0°$). Equations (4.4) have the following expressions

$$I_{TE}(0°) = \frac{\lambda^2}{4\pi r^2} x^6 \left| \left(\frac{\epsilon - 1}{\epsilon + 2} \right) + \left(\frac{\mu - 1}{\mu + 2} \right) \right|^2 \sin^2 \phi \tag{4.8}$$

$$I_{TM}(0°) = \frac{\lambda^2}{4\pi r^2} x^6 \left| \left(\frac{\epsilon - 1}{\epsilon + 2} \right) + \left(\frac{\mu - 1}{\mu + 2} \right) \right|^2 \cos^2 \phi \tag{4.9}$$

$I_{TE}(0°)$ and $I_{TM}(0°)$ are identically zero if the sum of the terms between bars is zero. In this case, the relation is not as trivial as it was for the previous one. Kerker et al analyzed this in detail and found [69] that if the optical properties (ϵ, μ) verified the following condition

$$\epsilon = \frac{4 - \mu}{2\mu + 1} \tag{4.10}$$

there is no scattering in the forward direction. In Figure 4.2 we include an example of the angular distribution of the scattered intensity for a dipole-like particle with optical properties,
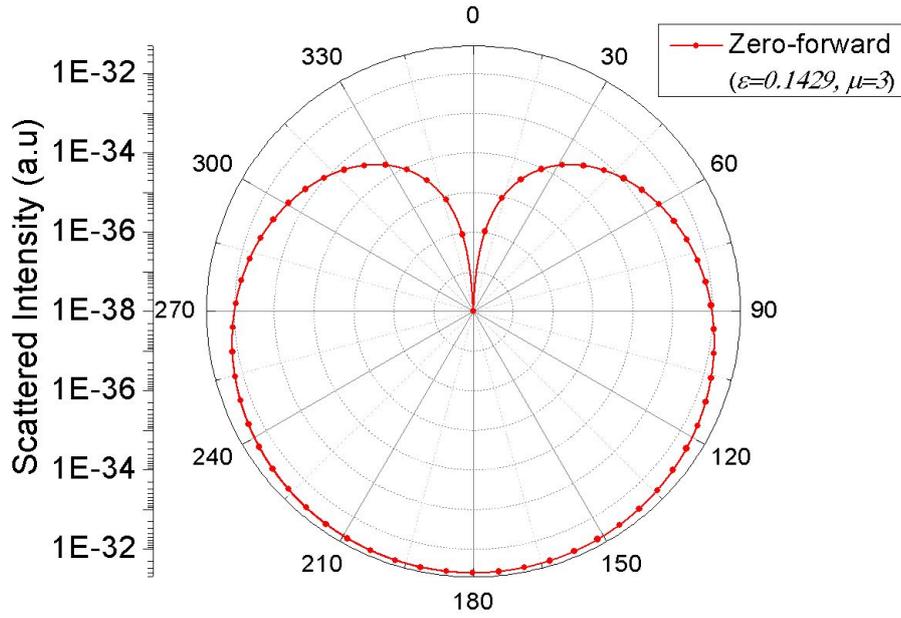
Figure 4.2: Scattering diagram for a dipole-like particle ($R = 10^{-6}\lambda$) with optical properties fulfilling the zero-forward condition and for a TM incident polarization (TE polarization is identical).

$(\epsilon, \mu) = (0.1429, 3)$, according to the zero-forward scattering condition (equation (4.10)).

4.2.3. Zero-Forward Scattering and the Optical Theorem

The optical theorem for spherical particles establishes that the extinction efficiency (Q_{ext}) and the scattering amplitude in the forward direction are related in the following way [14]

$$Q_{ext} = \frac{4}{x^2} Re\{S(0°)\} \tag{4.11}$$

When a spherical particle does not scatter in the forward direction, $S(0°)$ is zero and then, according to the optical theorem, the extinction efficiency should be equal to zero. The fact that $Q_{ext} = 0$ implies that the particle does not scatter neither absorbs electromagnetic radiation. This is only possible under the trivial condition that the optical constants of the particle and the surrounding medium match. Furthermore, in Figure 4.2, it can be seen that, in spite of $S(0°) = 0$, the particle scatters in other directions. This apparent paradox was studied some years ago [24]. Chýlek and Pinnick [24, 23] showed that the energy conservation conditions for a sphere demand that

$$|a_n|^2 \leq Re(a_n) \tag{4.12}$$

$$|b_n|^2 \leq Re(b_n) \tag{4.13}$$

It is easy to show that under the dipolar approximation (see equations (2.56) and (2.57)) and if the refractive index is real (there is not absorption), the scattering coefficients are imaginary and then the previous conditions are not fulfilled. Because of this, the Rayleigh approximation is characterized as a nonunitary approximation and the extinction efficiency cannot be calculated using equation (2.41) or the Optical Theorem. In this case, the extinction efficiency could be estimated using the relation

$$Q_{ext} = Q_{sca} + Q_{abs} \tag{4.14}$$

In a recent work [9], the authors stated that a simple modification of the approximate expression for the first two Mie coefficients can be used in order to comply the energy conservation requirements established by the Optical Theorem. They proposed adding the radiative correction [28] in such a way that the Mie coefficients, under the Rayleigh approximation, could be expressed as

$$a_1 = \left(-1 - \frac{3i}{2}x^3\frac{\epsilon + 2}{\epsilon - 1}\right)^{-1} \qquad b_1 = \left(-1 - \frac{3i}{2}x^3\frac{\mu + 2}{\mu - 1}\right)^{-1} \tag{4.15}$$

Taking into account these considerations, energy conservation is assured and, although the forward scattering is not zero, it is minimum with respect to other scattering angles.

4.2.4.   Identity TM-TE polarization under Kerker's Conditions

As it was mentioned above, the zero-backward and zero-forward scattering conditions proposed by Kerker et al [69] are based on the fact that the electric and the magnetic contributions to the total scattered intensity cancel each other. In this case, the switching from a TE to a TM polarization or viceversa has no effect on the overall scattering as it could be observed in some of the previous figures. If the electric and magnetic terms are not equivalent, the angular distributions of the scattered radiation differ completely from one polarization to the

other. To illustrate this, we plot in Figure 4.3 the scattering diagrams for a small particle for two different cases: in the first case the optical constants satisfy the zero-forward condition $(\epsilon, \mu) = (-5, -1)$ and in the second case they don't $(\epsilon, \mu) = (-3, -5)$. We see that the angular distributions for the first case (squares) are equal for both polarizations, but different for the second one.

4.3. Exception to the Zero-Forward-Scattering Theory

The theory proposed by Kerker et al. [69] has a trivial exception. When the particle has optical properties, relative to the surrounding medium, equal to 1, $(\epsilon, \mu) = (1, 1)$, this is particle and surrounding medium are equal, the zero-forward scattering condition is satisfied but the particle, as it is obvious, does not scatter in any direction.

However, this is not the only exception. We stated in [11] that another one occurs when the electric permittivity and the magnetic permeability are both equal to -2 ($\epsilon = \mu = -2$). In Figure 4.4, the polar distribution of the scattered intensity by a dipolar particle ($R = 10^{-6}\lambda$) and optical properties ($\epsilon = -2, \mu = -2$) is shown. The two incident polarizations are considered, with the incident electric field parallel (TM) or perpendicular (TE) to the scattering plane. Although the optical constants correspond to a double-negative or left-handed particle, they both hold Kerker's conditions: the zero-backward ($\epsilon = \mu$) and the zero-forward condition (Equation (4.10)). In spite of this the scattering diagram exhibits a maximum in the forward direction.

The explanation of this lies in the fact that two Mie resonances, an electric and a magnetic dipolar mode, appear simultaneously. In Figure 3.2(b), an electric dipolar and a magnetic dipolar resonance appear as two straight branches coinciding at $(\epsilon, \mu) = (-2, -2)$. The very high values that the scattering intensity attains, due to the excitation of those modes, make that the electric and magnetic contributions cannot be compensated in the forward direction anymore and hence the forward-scattering is not zero anymore. As a consequence, these values for the optical properties constitute an exception to the zero-forward-scattering condition.

This is a singular point. This means that only where the two resonances overlap, this singularity can be observed. For this reason, it should be analyzed only from a mathematical point of view and not as a real situation. In Figure 4.5, we plot the scattering diagrams for
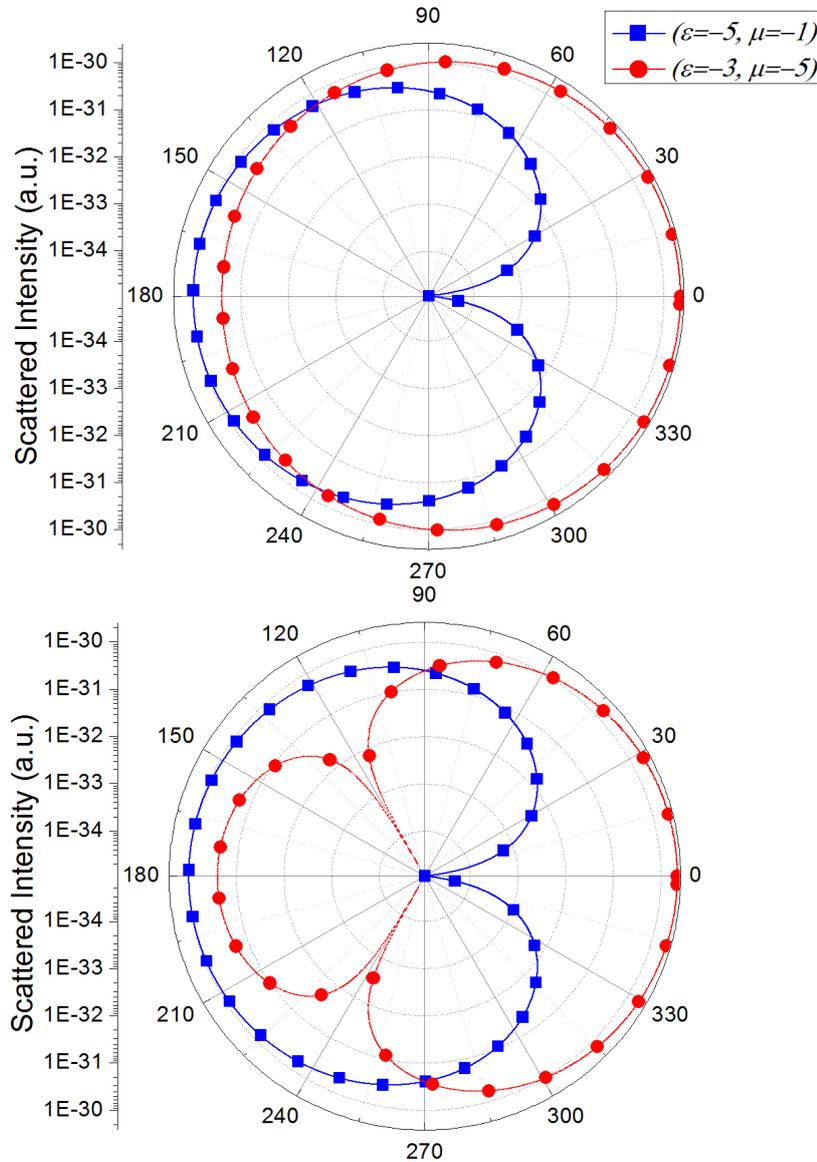
Figure 4.3: Scattering diagram for a particle with $R = 10^{-6}\lambda$ and optical constants fulfilling (squares) or not (circles) the zero-forward condition (equation (4.10)) for both incident polarizations:(a) TM and (b) TE
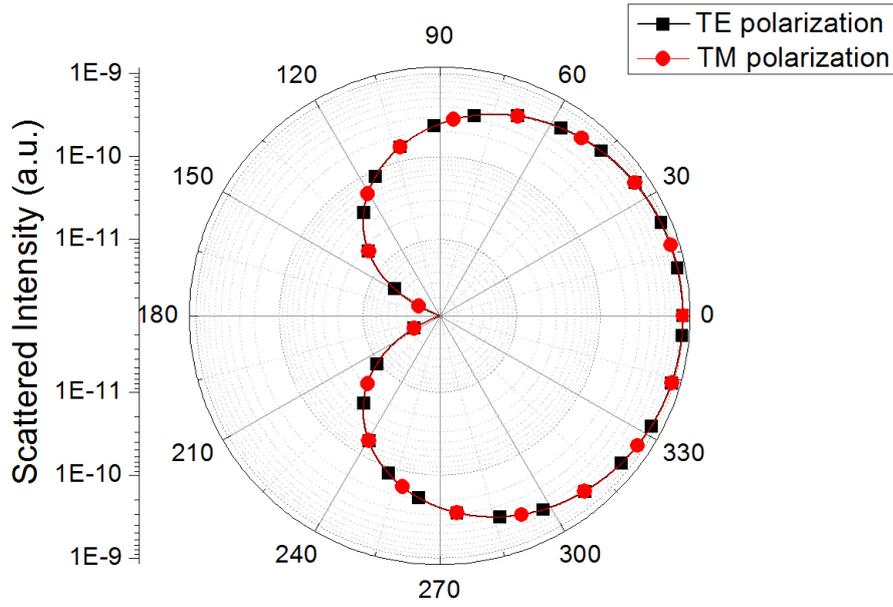
Figure 4.4: Scattering diagram for a very small particle ($R = 10^{-6}\lambda$) with optical properties $(\epsilon, \mu) = (-2, -2)$ and for both incident polarizations.

a dipole-like particle ($R = 10^{-6}\lambda$) for several values of the optical constants neighboring the exception $\epsilon = \mu = -2$. Every pair (ϵ, μ) fits the Kerker condition given by equation (4.10). The singular point $(\epsilon, \mu) = (-2, -2)$ is also included for comparison. Both incident polarizations, parallel (TM) and perpendicular (TE) to the scattering plane are considered. Although the values of the electric permittivity and the magnetic permeability are very close to those of the singular point, there is no scattered light in the forward direction as long as equation (4.10) is satisfied. With this figure, it can be concluded that the exception only appears for the intersection of the dipolar electric and the dipolar magnetic branches (Figure 3.2(b)).

4.4. Size effects on the Kerker's Conditions

Conditions for zero-forward or zero-backward scattering have been presented for dipole-like particles, but what happens when the particle size increases? In this section, we present the evolution of the Kerker's conditions as a function of the radius of the scatterer in order to analyze if the mentioned scattering features can still be observed. However, while finite, the considered particles are still very small compared with the incident wavelength.
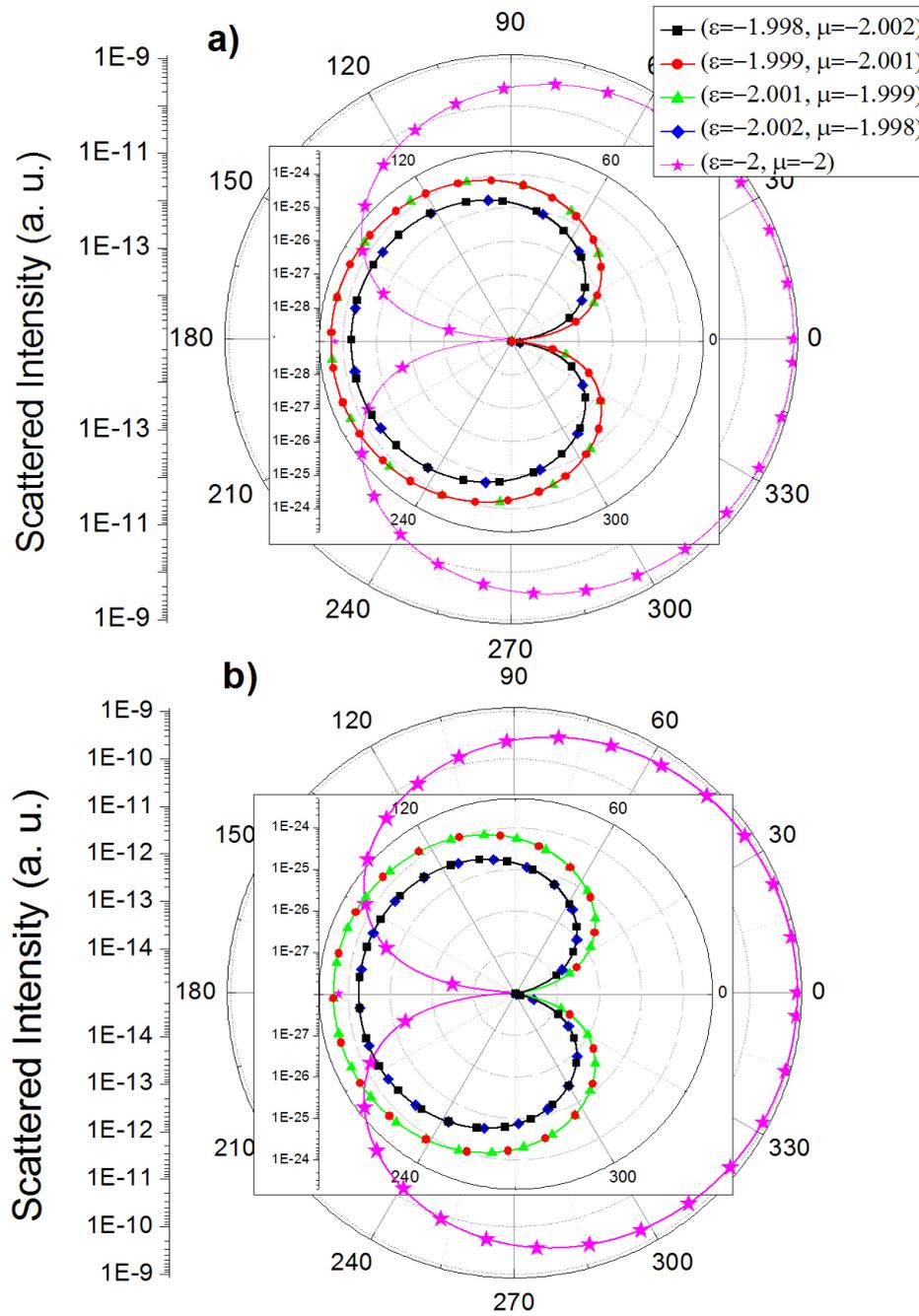
Figure 4.5: Scattering diagram for a very small particle ($R = 10^{-6}\lambda$) for both incident polarizations:(a) TM and (b) TE and for several pairs of values of the optical constants around $(\epsilon, \mu) = (-2, -2)$ that verify Kerker's condition for zero-forward scattering. $(\epsilon, \mu) = (-2, -2)$, the latter requiring the left general scale, which is huge in comparison with the rest.
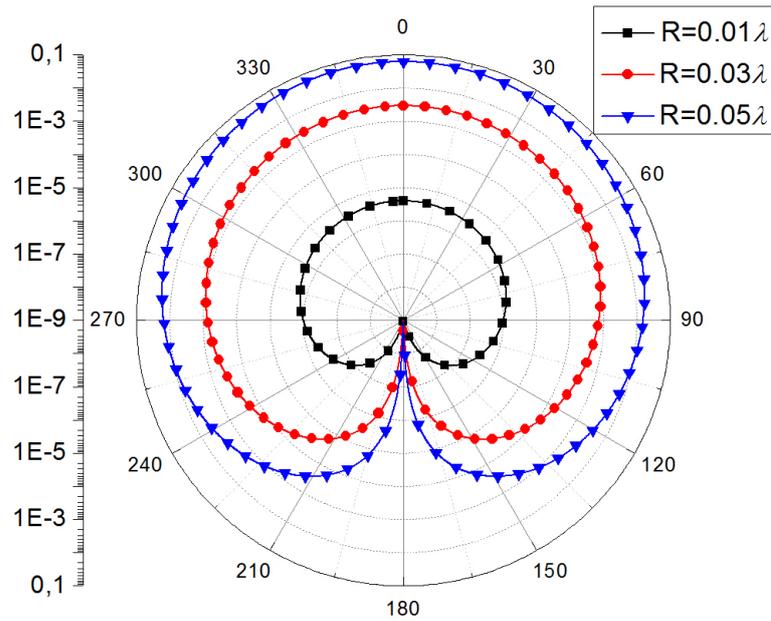
Figure 4.6: Polar scattering diagrams, in logarithmic scale, for a spherical particle with optical properties $(\epsilon, \mu) = (-3, -3)$ and illuminated by a TE-polarized incident light. Several particle sizes have been considered.

4.4.1. Influence of Particle Size on the Backward Direction

The zero-backward condition states that a particle with equal electric permittivity and magnetic permeability ($\epsilon = \mu$) does not scatter in the backward direction. Mathematically, it has been easy to demonstrate this statement for Rayleigh particles, but it is less easy to demonstrate it for finite-sized particles. In Figure 4.6, the scattering diagrams for an isolated particle, with optical properties in the negative range satisfying the zero-backward condition $(\epsilon, \mu) = (-3, -3)$ are plotted for several radius. The polar distribution of the scattered intensity is independent from the incident polarization, then we have only considered a TE-polarized incident beam. As can be seen, zero scattering in the backward direction is still observed for every particle size. This means that in this direction the electric and magnetic terms are compensated and then the zero-backward condition keeps for the analyzed range of R.

4.4.2. Influence of Particle Size on the Forward Direction

The influence of particle size on the zero-forward scattering condition is more complex than
for the previous case. As the scatterer grows, while obliging the optical constants to satisfy
the forward condition given by equation (4.10), the scattered intensity distribution in the
scattering plane starts to present non-null values in the forward direction. This is because
as R increases, the first two Mie coefficients acquire more complex expressions than the
ones given by equations (2.56), (2.57). Furthermore, higher order coefficients cannot be
neglected anymore. The electric and magnetic contributions to the far field differ in the
forward direction and cannot cancel each other. However, if the particle size is finite but still
very small compared with the incident wavelength, it is possible to find pairs (ϵ, μ) for which
light scattering in the forward direction is minimum.

As it was shown in Chapter 2, for values of $R \in [0.01\lambda, 0.05\lambda]$ (corresponding to the
nanometric range whan λ is in the visible part of the spectrum), the first four Mie coefficients,
a_1, b_1, a_2 and b_2, reproduce very accurately the scattered intensity by a sphere, which can be
written as

$$I_{TE} = \frac{\lambda^2}{4\pi r^2} \left| \frac{3}{2} \left(a_1 \pi_1(\cos\theta) + b_1 \tau_1(\cos\theta) \right) + \frac{5}{6} \left(a_2 \pi_2(\cos\theta) + b_2 \tau_2(\cos\theta) \right) \right|^2 \sin^2\phi$$

$$(4.16)$$

$$I_{TM} = \frac{\lambda^2}{4\pi r^2} \left| \frac{3}{2} \left(a_1 \tau_1(\cos\theta) + b_1 \pi_1(\cos\theta) \right) + \frac{5}{6} \left(a_2 \tau_2(\cos\theta) + b_2 \pi_2(\cos\theta) \right) \right|^2 \cos^2\phi$$

$$(4.17)$$

In Figure 4.7, the polar distribution of the scattered intensity for spherical particles of
different sizes is plotted. Different values of the electric permittivity and the magnetic per-
meability in the double-negative range ($\epsilon < 0, \mu < 0$) were chosen such that a minimum
in the forward direction, with respect to the other scattering angles, appears. These values
are summarized in table 4.1. The incident beam is linearly polarized with the electric field
perpendicular to the scattering plane, this is a TE polarization. A TM incident polarization
produces similar distributions, according to the TE-TM identity characteristic explained be-
fore. We have chosen the negative-negative range for the optical constants. However, other
similar pairs can be obtained for other ranges. For low values of *R*, the scattered intensity in
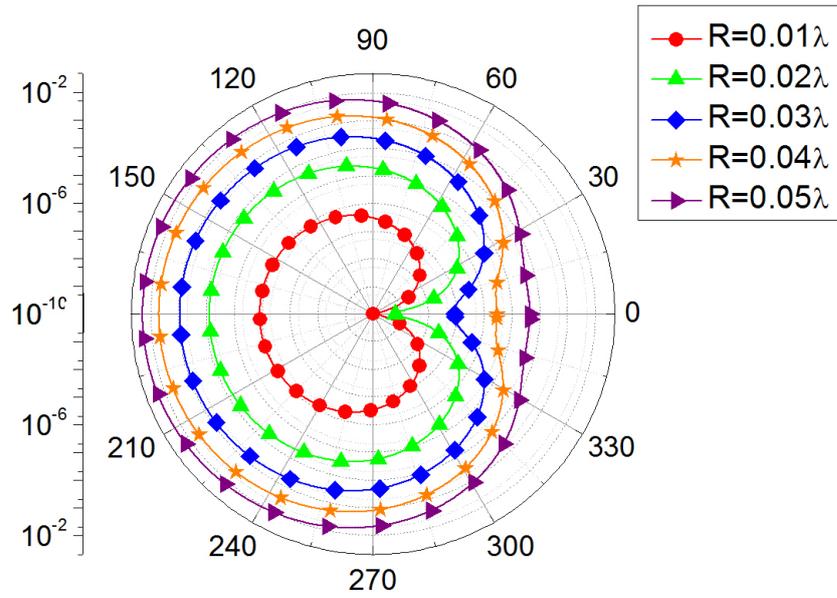
Figure 4.7: Polar scattering diagrams, in logarithmic scale, for a spherical particle illuminated with a TE linearly polarized incident beam. For each particle size, optical properties, in the negative-negative range, are such that the scattered intensity is minimum in the forward direction. Table 4.1 summarizes the values for each particles size.

the forward directions is considerably smaller compared with other angles. As *R* increases, the minimum becomes less pronounced. This occurs due to the increasing influence of the quadrupolar terms, a_2 and b_2, especially for $R > 0.03\lambda$.

At this point, we have shown that, though non zero-forward scattering can be obtained for finite-size particles, it is possible to find pairs (ϵ, μ) for which forward scattering is minimum. The obvious next step is to analyze whether these pairs fulfill or not the zero-forward condition or other similar mathematical relation. For this purpose, in Figure 4.8 the magnetic permeability is plotted versus the electric permittivity, in such a way that each point of the figure corresponds to a minimum in the forward scattering for an incident TE polarization. Several particle sizes are considered to analyze the evolution of that minimum with *R*. These minima are obtained searching the minimum of the scattered intensity (Equation (4.16)) in the forward direction for the same range of ϵ and μ. This range is $[-0.1, -8]$ with a grid-space equal to 0.005. The values are chosen in the negative-negative range because more interesting scattering features occur in this interval, as we showed in Chapter 3. This study can be generalized for other ranges and similar results would be obtained. It must be remarked that some discontinuities are observed around $\epsilon(\mu) = -2$ and $\epsilon(\mu) = -1.5$. These are due

$\mathbf{R} \setminus \lambda$	ϵ	μ
0.01	-1.06	-4.55
0.02	-1.07	-4.55
0.03	-1.09	-4.55
0.04	-1.11	-4.55
0.05	-1.13	-4.55

Table 4.1: Pairs of values for the optical constants (ϵ, μ as a function of the particle size for which light scattering presents a minimum in the forward direction as shown in Fig. 4.7

to the excitation of the electric (magnetic) dipolar and quadrupolar resonances appearing for these values, respectively. The resonant behavior produces an important enhancement of the scattered intensity and several changes in its polar distribution.

As can be seen in Figure 4.8, the pairs (ϵ, μ) which produce a minimum scattered intensity in the forward direction follow a relation similar to the one proposed by Kerker et al [69] for dipole-like particles (included in the figure for comparison). However, as the particle size increases the calculated pairs are increasingly shifted from the Kerker's relation. For this reason, we fitted our results to an expression similar to equation (4.10) letting the coefficients depend on the radius of the particle.

$$\mu = \frac{b(R) + c(R)\epsilon}{a(R)\epsilon + 1} \tag{4.18}$$

While equation (4.10) is symmetric with respect to a $\epsilon - \mu$ interchange, this symmetry tends to disappear as the particle size increases. After checking both forms (ϵ as a function of μ or viceversa), we can conclude that equation (4.18) is the best option.

In Figure 4.9, the fitting coefficients are plotted as a function of the radius of the particle. For very small particles, the values are not far from those given by equation (4.10) [69]. However, as the scatterer grows, the differences between the small-particle limit values and the fitted ones become bigger. Their evolutions are similar: as R increases, the values of the coefficients tend to lower values or to more negative values in the case of $c(R)$. However $c(R)$ does not change as much as $a(R)$ or $b(R)$, with a variation around 2.5% while the others change around 10% in the considered range of R. The evolution of these coefficients can be related with the resonance's shift as particle size changes, which was explained in Chapter 3. Analyzing in detail the expressions for the forward scattering, it can be observed
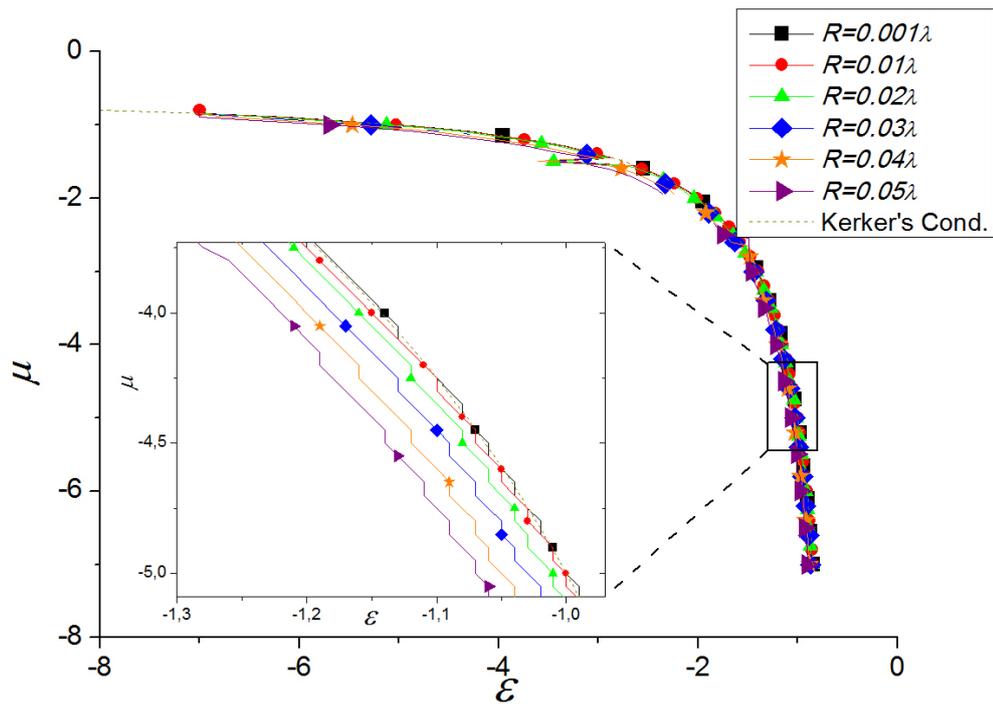
Figure 4.8: Pairs (ϵ, μ) for which the forward scattered intensity of a sphere is minimum for several values of the radius. For comparison, Kerker's conditions for dipole-like particles $(R \rightarrow 0)$ is also included as a dashed line. A magnified inset shows the evolution clearly

.
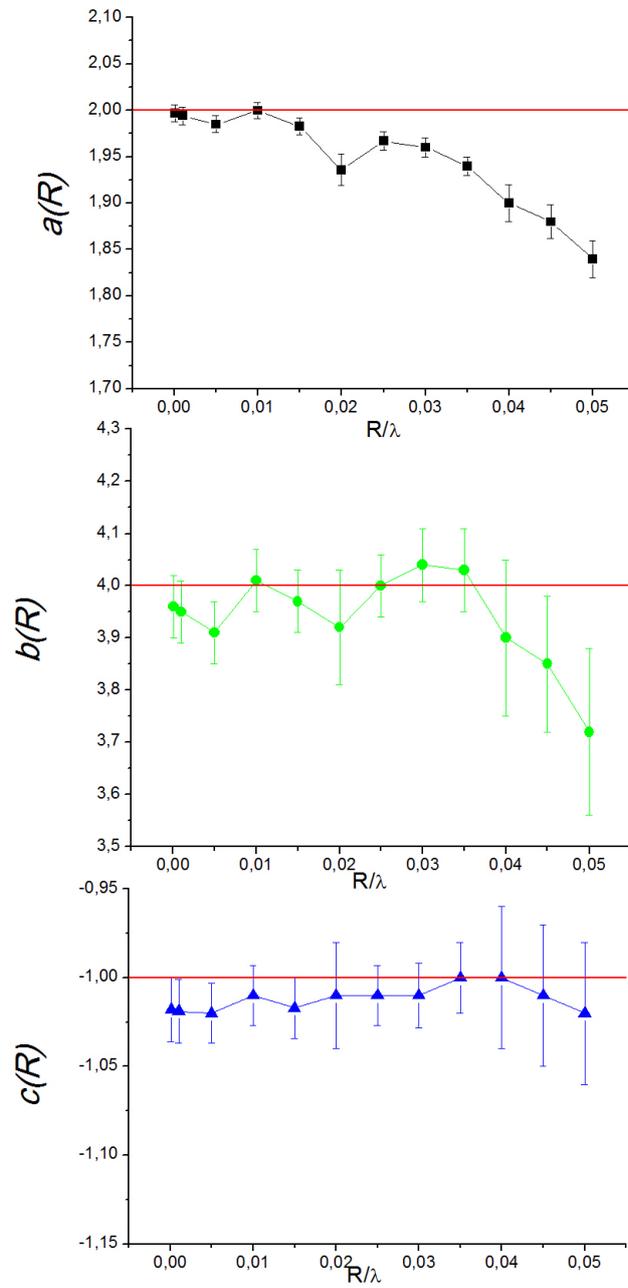
Figure 4.9: Evolution of the fitting coefficients (Eq. (4.18)) for the pairs (ϵ, μ) which minimize forward scattering (TE polarization). Solid lines correspond to the values of the Kerker et al. condition [69]

.

that the coefficients $a(R)$, $b(R)$ and $c(R)$ depend on the spectral position of the electric, electric+magnetic and magnetic dipolar resonances, respectively. Then, we can relate the pronounced evolution of $a(R)$ with the high sensitivity of the electric dipolar resonance with particle size (Figure 3.5), while the magnetic mode is less sensitive in this size range producing an almost constant evolution of $c(R)$. Finally, the combination of electric and magnetic resonances' evolution give a smooth change of $b(R)$ with R.

All these results were calculated for a linearly polarized incident beam with the electric field perpendicular to the scattering plane (TE polarization). As it was showed above, the same behaviors can be observed if the incident beam is polarized with the electric field parallel to the scattering plane (TM polarization).

4.5. Generalization of the Minimum Light Scattering for other Scattering Angles

A general analysis of the polar distribution of the scattered intensity by a particle with optical constants in the double-negative range ($\epsilon < 0, \mu < 0$) suggests the possibility of extending the previous study to other scattering angles. Choosing certain angles different from $0°$ and $180°$, we have found pairs (ϵ, μ) which produce a minimum scattered intensity with respect to other angles within the scattering plane. As an example, in Figure 4.10, we plot the scattering diagrams of a very small spherical particle ($R = 0.01\lambda$) illuminated by a TE polarized incident beam. The optical constants are in the double-negative range in such a way that light scattering reaches a minimum at representative angles like $30°$, $60°$,$120°$ and $150°$. Each diagram shows a double-lobe structure with the position of the minimum depending on the particular values of the electric permittivity and the magnetic permeability. By tuning the optical constants of the material, the minimum position in the scattered intensity can be changed.

The curves of Figure 4.10 are symmetric with respect to the forward-backward direction, because of that we have limited our analysis to the upper hemisphere (from $0°$ to $180°$).

The existence of these pairs (ϵ, μ) that minimize light scattering at scattering angles different from $0°$ and $180°$ allow to extend the previous study, made for $\theta = 0°$, to these other angles. Figure 4.11 summmarizes the results we found. The pairs (ϵ, μ) that produce minimum light scattering at: (a) $30°$, (b)$45°$, (c)$60°$, (d)$120°$, (e)$150°$ and (f) $170°$ were obtained in the negative-negative range ($\epsilon \in [-0.1, -8], \mu \in [-0.1, -8]$ with a grid-space equal to
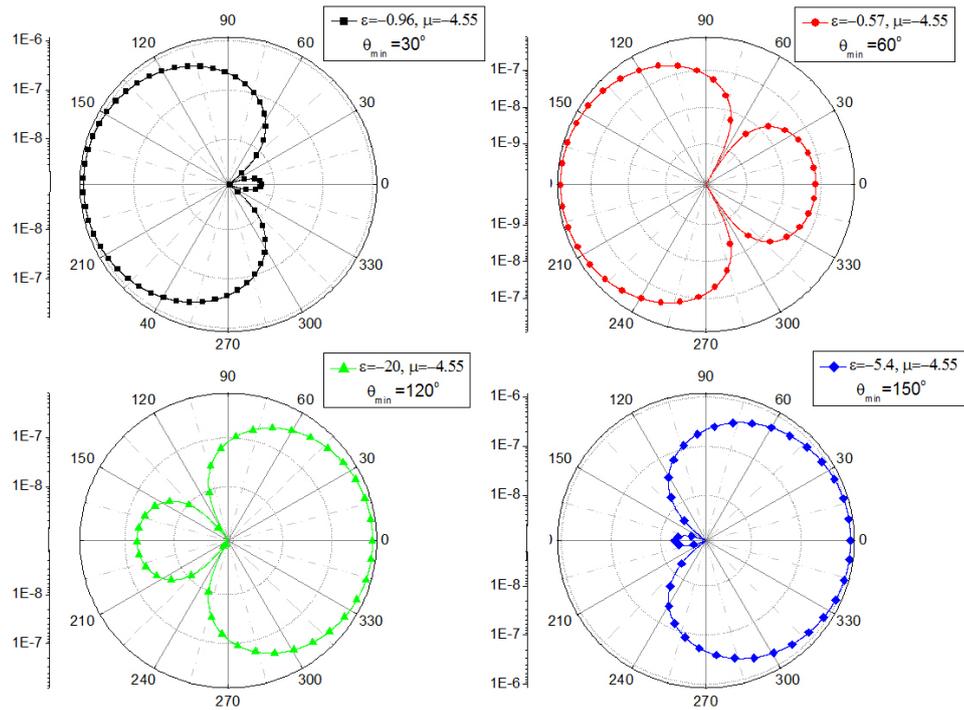
Figure 4.10: Polar diagrams of the scattered intensity for a spherical particle with $R = 0.01\lambda$ and optical constants in the negative-negative range (labeled in the figure) which produce a minimum scattering at certain scattering angles. The particle is illuminated with a linearly polarized incident plane wave with the electric field perpendicular to the scattering plane (TE polarization)
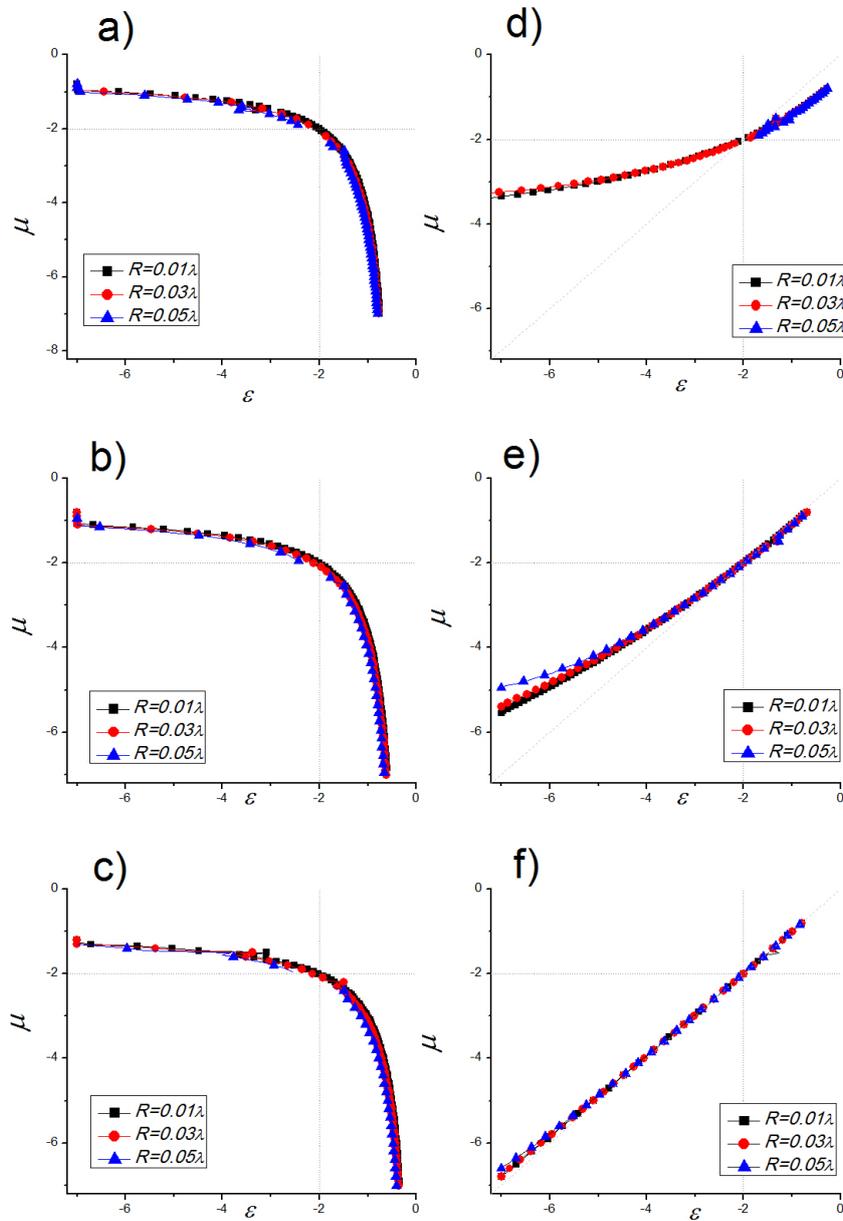
.

Figure 4.11: Pairs (ϵ, μ) which produce minimum light scattering at: (a) 30°, (b)45°, (c)60°, (d)120°, (e)150°, (f)170°. Several particle sizes are considered. The position of the electric and magnetic dipolar resonances for a dipole-like particle $((\epsilon, \mu) = (-2, -2)$, respectively) are plotted in each figure. Also the bisection ($\epsilon = \mu$) has been included for $\theta = 120°, 150°$ and 170°. TE incident polarization has been considered.

0.005). Different values of the radius of the particle are considered in order to analyze also the evolution of the curves with particle size. Two different behaviors can be identified. The pairs for which light scattering is minimum at $30°$, $45°$ or $60°$ follow a relation similar to those corresponding to the forward direction and can be fitted to an equation like equation (4.18). Although for large scattering angles the agreement is poor and other expressions are more suitable, we can conclude that the optical constants (ϵ, μ) which produce minimum light scattering in the forward hemisphere $(-90° < \theta < 90°)$ evolves following a relation like equation (4.18). On the other hand, pairs which produce minimum light scattering in the backward hemisphere $(90° < \theta < 270°)$ cross the point (-2,-2) with a positive slope, as can be seen in Figure 4.11 (d), (e) and (f). The tendency, in this region, is that as the scattering angle increases, the curves tend to the relation $\epsilon = \mu$, that is the zero-backward condition proposed by Kerker et al [69].

The transition between the two behaviors is smooth, reaching an intermediate behavior at $90°$. The curve corresponding to minimum light scattering at $90°$ is unique because these minima appear for a combination $\epsilon - \mu$ at which the particle scatters like an electric or a magnetic dipole depending on the incident polarization (TM or TE respectively).

The curves are not strong size-dependent, as can be observed. Still, it is interesting to remark that the curves in the backward hemisphere are more sensitive to particle size than those in the forward hemisphere. However, as the scattering angle approaches $180°$ the sensitivity decreases. It can be seen that the influence of the electric and magnetic dipolar resonances is still observed and each curve presents a discontinuity at $(\epsilon = \mu = -2)$.

As before, the results, presented in Figure 4.11, for scattering angles different from $0°$ and $180°$ correspond to an incident polarization with the electric field perpendicular to the scattering plane. If we repeat this complete study with a TM polarization, this is, with the incident electric field parallel to the scattering plane, the pairs (ϵ, μ) follow the behavior plotted in Figure 4.12.

While for the cases of $\theta = 0°$ or $\theta = 180°$, the two orthogonal polarizations produce similar results when the scattering angle differs from these values the difference between TE and TM polarizations increases, as can be seen. In order to analyze this in more detail, in Figure 4.13 we plot, as a comparison, the pairs (ϵ, μ) that minimize light scattering for a sphere $(R = 0.03\lambda)$ at some of the scattering angles considered previously and for both polarization states. For scattering directions different from the forward or the backward one, the pairs that minimize light scattering differs for both polarizations except in the surroundings of $(\epsilon = \mu = -2)$ where the differences become negligible. As we have mentioned several times through this chapter, in the vicinity of this point, depending on the particle size, the
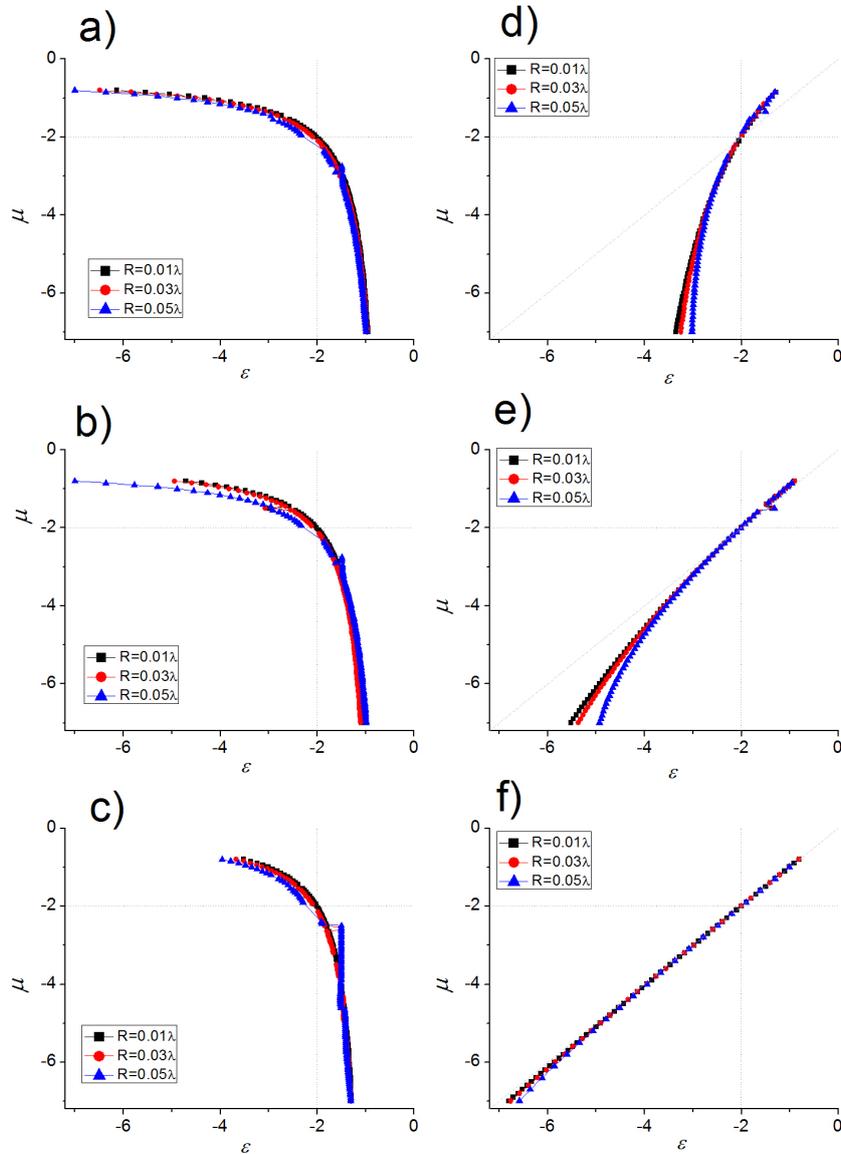
Figure 4.12: Pairs (ϵ, μ) which produce minimum light scattering at: (a) $30°$, (b)$45°$, (c)$60°$, (d)$120\circ$, (e)$150°$, (f)$170°$. Several particle size are considered. The position of the electric and magnetic dipolar resonances for a dipole-like particle($\epsilon = -2$ and $\mu = -2$, respectively) are plotted in each figure. Also the bisection ($\epsilon = \mu$) has been included for $\theta = 120°, 150°$ and $170°$. TM incident polarization has been considered
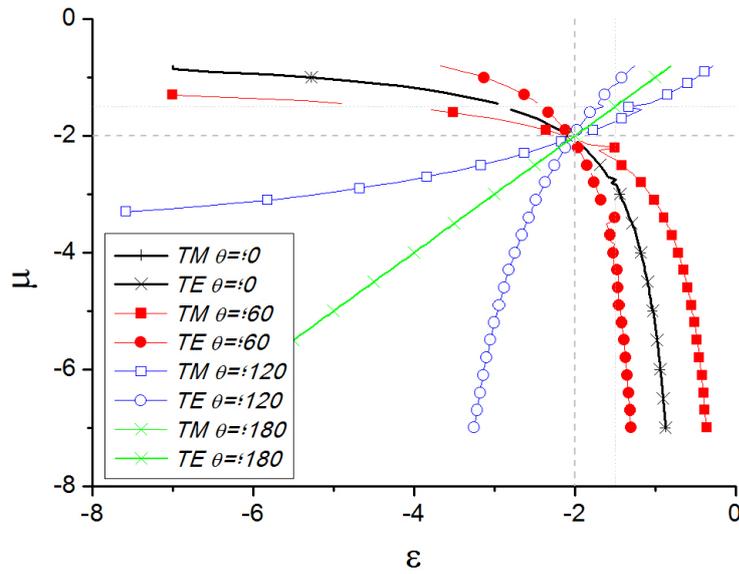
Figure 4.13: Double-negative (ϵ, μ) pairs that minimize light scattering at certain scattering angles ($0°$, $60°$,$120°$ and $180°$) for a spherical particle of radius $R = 0.03\lambda$ and for TM (circles) and TE (squares) incident polarization. The dipolar (dashed lines) and the quadrupolar (dotted lines) electric and magnetic resonances are labeled because their appearance produce discontinuities in the curves.

electric and magnetic dipolar resonances are excited. When this occurs, the two orthogonal contributions to the scattered intensity (Equation (4.4)) tends to be equivalent and then by switching from TE to TM, or viceversa, no effect is produced in the overall scattering. However, at the exact point where the resonances match, light scattering is not minimum and the curves are discontinuous.

4.6. Conclusions

The control of the direction of the scattered electromagnetic radiation of a certain scatterer could be quite useful for futuristic applications, for instance optical communications. The first studies about this control were performed by Kerker et al [69] where light scattering of a dipole-like particle could be suppressed either in the forward or the backward direction by tunning its optical constants. This chapter has been devoted to the analysis of these conditions, from which we have obtained interesting results. Some of them are summarizes as follows.

- It has been checked that under Kerker's conditions there is a TE-TM identity. That is, the switching from a perpendicular to a parallel incident polarization does not produce any change in light scattering.

- The zero-forward condition involves an apparent paradox with the Optical Theorem. However, this paradox can be easily explained from a mathematical point of view. Chýlek and Pinnick showed that the dipolar approximation used by Kerker et al is a non-unitary approximation and hence the Optical Theorem cannot be applied [24]. In addition, Alù and Engheta stated that by including the radiative correction [28] to the Mie coefficients the energy conservation is assured under the zero-forward condition.

- The zero-forward condition has an important exception when $(\epsilon, \mu) = (-2, -2)$. For these values of the optical constants, two dipolar resonances, one electric and one magnetic, are excited. This produces that the electric and the magnetic contributions cannot be compensated each other and high amounts of electromagnetic radiation are detected in the forward direction.

Kerker's conditions were enunciated for dipole-like particles, this is $R \to 0$. We have also wanted to observe the evolution of these conditions as particle size increases, and even if similar conditions can be deduced for other scattering angles different from $0°$ and $180°$. From this analysis, these are the main conclusions:

- As particle size increases in a range $R \in [0.01, 0.05]\lambda$, minimums on the scattered intensity, instead of zeros, can be observed for certain pairs (ϵ, μ) either on the forward, the backward or other scattering directions.

- While the minimum in the backward direction is more stable as R increases, the one on the forward direction becomes strongly less sharp with the size.

- The zero-backward condition proposed by Kerker et al ($\epsilon = \mu$) is still representative for the pairs (ϵ, μ) producing minimum scattered intensity in the backward direction when particle size is in the considered range. On the contrary, while the zero-forward conditions (equation (4.10)) reproduce the behavior of the pairs (ϵ, μ) minimizing the forward light scattering, it does not fit with the values. A similar equation to equation (4.10) but with their parameters depending on R is proposed. This new curve reproduce accurately both the behavior and values of the optical constants.

- We have obtained pairs (ϵ, μ) for which the scattered intensity is minimum at different scattering angles in the upper hemisphere $(0° < \theta < 180°)$. The symmetry of the scatterer involves that similar results should be obtained for the bottom hemisphere.

- For scattering angles in the forward hemisphere $(-90° < \theta < 90°)$, the pairs (ϵ, μ) that minimize the scattered intensity follow a similar behavior as that described by equation (4.10). If the scattering angles are in the backward hemisphere $(90° < \theta < 270°)$ the curves have a positive slope and tend to the zero-backward condition as the scattering angle approaches to $180°$. The evolution from one to other behavior is smooth with an intermediate behavior at $90°$.

- As in the forward and backward cases, pairs (ϵ, μ) minimizing scattered intensity at different scattering angles depend slightly on particle size. However, while pairs are polarization-independent for the forward and backward cases, for different scattering angles these pairs are different depending on the incident polarization.